Study of Jenkins Model with porosity on a rotating disk

G. R. Meghashree[1], C. S. Asha[2] and L.N. Achala[3]

[1]Research Scholar, [2]Assitant Professor, [3]Head and Coordinator,
P.G. Department of Mathematics and Research Centre in Applied Mathematics
M.E.S. College of Arts, Commerce and Science, 15th cross, Malleswaram, Bengaluru-560003.
Email ID: [1]meghashree01@gmail.com, [2]csasharukmini@gmail.com, [3]anargund1960@gmail.com.

Absract: The flow of a ferrofluid over a rotating disk with porosity is investigated through Jenkins model. In this model the magnetization and applied magnetic fields are collinear and we consider the co-rotational derivative of magnetization through which a material constant is introduced. The governing equations are solved by Cochran series approximations. The variation in porosity shows the fluctuation in velocity and pressure where as variation in material constant has a prominent effect on radial velocity and pressure but negligible effect on tangential velocity and axial velocity. The calculated values are compared to show the effect of porosity and material constant on a ferrofluid flow.

Keywords: Ferrofluid, Material constant, Porosity, Magnetic field, Rotating disk.

1.INTRODUCTION

Ferrofluid is a synthesized fluid developed in early 1960's by dispersing ferrimagnetic or ferromagnetic particles which are of size $3-10nm$ into the solvents(polar or non-polar). Here the particles are coated with a molecular layer of a dispersant/surfactant in order to avoid clustering/agglomeration and its flow and energy is controlled by external magnetic field. Ferrofluid works on the concept called ferromagnetism. Ferromagnetism involves the study of spin magnetic moments[1, 2, 3]. In the year 1963, Steve papell invented ferrofluid by the method of size reduction to create liquid rocket fuel that could be drawn towards a fuel pump in a weightless environment by applying magnetic feild. Further the ferrofluid was processed by Rosensweig through chemical precipitation. Ferrofluids have application in the field of Industry, Engineering, Medical etc. The presence of ferrofluid in a loudspeakers improve heat transfer from coil to the surrounding and hence improving the performance of loudspeakers. Ferrofluids have the capability of reducing friction hence making them useful in variety of electronic and transportation

applications. It is used as pressure seals in compressors, blowers, computer hard - drivers and lasers etc. In the field of medicine it is used for magnetic drug targeting, nano surgeries, X-ray machines and MRI scans[4]. Currently ferrofluids are used to create an artificial heart in which heart is surrounded by magnets, the ferrofluid fixed to frame of the heart will expand and contract when needed, imitating the pumping of real heart.

Ferrofluids are analysed through three models Neuringer - Rosensweig model, Jenkins model and Shliomis model. Neuringer - Rosensweig model explains the magnetization and magnetic field are collinear and stress tensor is symmetric. Jenkins model involves the co-rotational derivative of magnetization. In Shliomis model the magnetization and magnetic field are not collinear and stress tensor is asymmetric. Paras Ram et al.[5, 6, 7] studied the effect of porosity on ferrofluid flow, axi-symmetric ferrofluid flow and revovling ferrofluid on a rotating disk using Neuringer - Rosensweig model. The obtained non - linear partial differential equations are reduced to non - linear ordinary differential equations by using the well known Von Karman transformations[8]. The solution to the problem is obtained by Cochran[9] asymptotic series and comparision is done with the work of Benton[10] to analyse the effect of porosity. Verma and Singh [11] analysed that, involvement of porous annulus in the cylindrical tubes decreases the flow at inner wall and accelerates the flow at outer wall of tubes in axial direction. Attia[12] studied the effect on velocity, by considering the steady incompressible viscous non-Newtonian fluid on a porous disk with heat transfer under uniform rotation. Paras Ram and Anupam Bhandari[13] studied the effect of porosity with variable viscosity on a flow characterstics of revolving fluid. Attia[14] analysed the effect of porosity on a unsteady Couette flow and showed that increase in the porosity decreases the velocity, viscous dissipation and temperature. Paras Ram and Kushal Sharma[15] showed in a porous medium the velocity components in radial and tangential directions tend to zero faster with the presence of magnetic field dependent viscosity. Anupam Bhandari and Vipin Kumar[16] analysed that porosity as more influence on velocity profile in comparison to magnetic field dependent viscosity. Pouya Barnoon et al.[17] presented that rate of heat transfer changes with varying porosity in the presence of magnetic field.

Shah and Bhat[18] derived equations under Jenkins model in the study of ferrofluid lubrication of a slider bearing and discussed the effect of material constant on pressure, load

capacity and friction force. Paras ram and Vedan[19] proved that their is increase in the load capacity under Jenkin's model in comparison to the work of Agarwal[20] in which the material constant was not considered for inclined slider bearing. Rajesh and Bhat[21] studied the load capacity of ferrofluid lubrication by varying the radial permeability, axial permeability, rotation of plates and also discussed the response time of the ferrofluid in each case. Mishra et al.[22] studied the involvement of space dependent magnetic field results in increase of pressure and load capacity. Patel and Deheri[23] studied the effect of slip velocity on a curved rough annular squeeze film which mentions that slip velocity help to reduce friction leading to effective performance of a bearing system. Asha and Achala[24] showed that for rough and smooth slider bearing the load capacity decreases and increases with and without squeeze velocity respectively.

Here we consider the Jenkins model which is the generalization of Neuringer - Rosensweig model. The Jenkins model alters both velocity and pressure where as the Neuringer - Rosensweig model alters pressure alone[22]. Paras Ram et. al.[4] has studied the porosity effect on ferrofluid flow with rotating disk through Neuringer - Rosensweig model. We extend this work for Jenkins model with porosity on a rotating disk. The paper is divided into four sections, section 1 consists of introduction, section 2 consists governing equations of the problem, section 3 has mathematical formulation and details of solution, section 4 contain results and discussions and section 5 contain graphs.

2. GOVERNING EQUATIONS

We consider the steady symmetric flow of an incompressible ferrofluid over a rotating disk with porosity through Jenkins model, with vertical axis being axis of rotation. The rotationally symmetric nature of the flow indicates that the velocity components and pressure in cylindrical components are independent of angular coordinates and angular velocity ω is considered to be uniform at large distance from plate. This model considers the magnetization , applied magnetic fields as collinear and existence of co-rotational derivative of magnetization. The governing equations and geometric model are as follows:

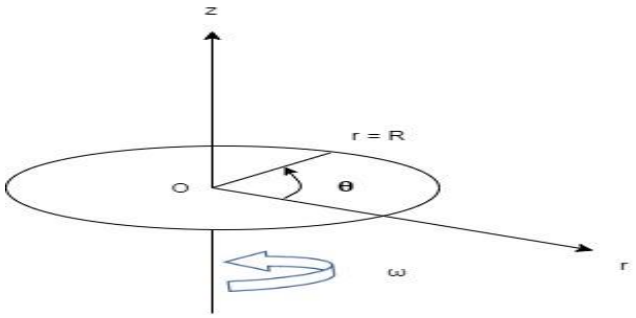

Figure 1: Ferrofluid flow with rotating disk

Equation of continuity for incompressible fluid is,

$$\nabla \cdot \vec{q} = 0, \tag{1}$$

Equation of motion of ferrofluid for Jenkins model is,

$$\frac{\rho}{\epsilon^2}[(\vec{q} \cdot \nabla)\vec{q}] = -\nabla p + \frac{\mu_f}{\epsilon}\nabla^2\vec{q} + \mu_0(\vec{M} \cdot \nabla)\vec{H} - \nabla\psi + \frac{\rho\beta^2}{2\epsilon}\nabla \times \left(\frac{\vec{M}}{M} \times (\nabla \times \vec{q}) \times \vec{M}\right), \tag{2}$$

Maxwell's Equations are

$$\nabla \times \vec{H} = 0, \tag{3}$$

$$\nabla \cdot (\vec{H} + 4\pi\vec{M}) = 0, \tag{4}$$

$$\vec{M} = \overline{\mu}\vec{H}, \tag{5}$$

$$\overline{\mu} = \frac{\mu_f}{\mu_0} - 1, \tag{6}$$

$$\vec{M} \times \vec{H} = 0. \tag{7}$$

Where $\vec{q}$ is velocity of ferrofluid, $\vec{H}$ is Magnetic field intensity, $\vec{M}$ is magnetization, p is fluid pressure, $\overline{\mu}$ is the magnetic susceptibility, μ_f is fluid viscosity, μ_0 is magnetic permeability of free space, ρ is fluid density, ψ is velocity potential, β is material constant and ϵ is the porosity.

3 MATHEMATICAL FORMULATION AND SOLUTION

We are analyzing the system for two cases of magnetic fields as follows,

Consider $\vec{q} = (v_r, v_\theta, v_z)$, $\vec{H} = (H_r, H_\theta, H_z)$ and $\vec{M} = (M_r, M_\theta, M_z)$

Case 1 : The constant magnetic field in radial direction.

That is $\vec{H} = (H_0, 0,0)$

Considering the above assumptions, equations (1) and (2) can be written in cylindrical form as follows:

$$-\frac{1}{\rho}\frac{\partial p}{\partial r} - \frac{H_0\beta^2\overline{\mu}}{2\epsilon}\left[\frac{\partial^2 v_r}{\partial z^2} - \frac{\partial^2 v_z}{\partial z \partial r}\right] + \frac{\nu}{\epsilon}\left[\frac{\partial^2 v_r}{\partial r^2} + \frac{\partial}{\partial r}\left(\frac{v_r}{r}\right) + \frac{\partial^2 v_r}{\partial z^2}\right] = \frac{1}{\epsilon^2}\left[v_r\frac{\partial v_r}{\partial r} + v_z\frac{\partial v_r}{\partial z} - \frac{v_\theta^2}{r}\right], \quad (8)$$

$$-\frac{H_0\beta^2\overline{\mu}}{2\epsilon}\left[\frac{\partial^2 v_\theta}{\partial r^2} + \frac{\partial}{\partial r}\left(\frac{v_\theta}{r}\right)\right] + \frac{\nu}{\epsilon}\left[\frac{\partial^2 v_\theta}{\partial r^2} + \frac{\partial}{\partial r}\left(\frac{v_\theta}{r}\right) + \frac{\partial^2 v_\theta}{\partial z^2}\right] = \frac{1}{\epsilon^2}\left[v_r\frac{\partial v_\theta}{\partial r} + v_z\frac{\partial v_\theta}{\partial z} + \frac{v_r v_\theta}{r}\right], \quad (9)$$

$$-\frac{1}{\rho}\frac{\partial p}{\partial z} + \frac{H_0\beta^2\overline{\mu}}{2\epsilon}\left[\left(\frac{\partial^2 v_r}{\partial r \partial z} - \frac{\partial^2 v_z}{\partial r^2}\right) + \frac{1}{r}\left(\frac{\partial v_r}{\partial z} - \frac{\partial v_z}{\partial r}\right)\right] + \frac{\nu}{\epsilon}\left[\frac{\partial^2 v_z}{\partial r^2} + \frac{1}{r}\frac{\partial v_z}{\partial r} + \frac{\partial^2 v_z}{\partial z^2}\right] = \frac{1}{\epsilon^2}\left[v_r\frac{\partial v_z}{\partial r} + v_z\frac{\partial v_z}{\partial z}\right], \quad (10)$$

$$\frac{\partial v_r}{\partial r} + \frac{v_r}{r} + \frac{\partial v_z}{\partial z} = 0. \quad (11)$$

Here v_r, v_θ, v_z, M_r, M_θ, M_z, H_r, H_θ and H_z are the radial, tangential and vertical components of velocity, magnetization and magnetic field respectively. It is considered that the fluid is revolving with uniform angular velocity ω at large distance from the disk. Due to the rotation of an infinitely long disk the initial and boundary approximation of the flow is considered as follows

$$\begin{cases} \text{at} \quad z = 0; \quad v_r = 0, \quad v_\theta = r\omega, \quad v_z = 0, \\ \text{at} \quad z = \infty; \quad v_r = 0, \quad v_\theta = 0, \quad v_z \quad \text{tends to a finite negative value} \end{cases} \quad (12)$$

The system of equations $(8) - (11)$ are transformed to ordinary differential equations by using Von Karman transformations [8] for a rotating disk which are as follows:

$$v_r = r\omega E(\alpha), \quad v_\theta = r\omega F(\alpha), \quad v_z = \sqrt{\nu\omega}G(\alpha), \quad p = \rho\omega\nu P(\alpha) \quad \text{where} \quad \alpha = z\sqrt{\frac{\omega}{\nu}}. \quad (13)$$

The system considered has no rotation at large distance from z thus the pressure is independent of r, where ω is the rotation, ν the kinematic viscosity, α is the dimensionless parameter of z.

The reduced ordinary differential equations are given by,

$$\epsilon[1-\overline{\beta}]E'' - E^2 + F^2 - GE' = 0, \tag{14}$$

$$\epsilon F'' - GF' - 2EF = 0, \tag{15}$$

$$\epsilon^2 P' - \epsilon G'' - 2\overline{\beta}\epsilon E' + GG' = 0, \tag{16}$$

$$G' + 2E = 0. \tag{17}$$

From equation (12), we get boundary conditions as below

$$E(0) = 0, F(0) = 1, G(0) = 0, E(\infty) = 0, F(\infty) = 0, G(\infty) = -c. \tag{18}$$

The system of equations $(14) - (17)$ are expanded through Cochran asymptotic expansion [9], which are

$$E \approx \sum_{n=1}^{\infty} a_n e^{\left(-\frac{c\alpha n}{\epsilon}\right)}, \tag{19}$$

$$F \approx \sum_{n=1}^{\infty} b_n e^{\left(-\frac{c\alpha n}{\epsilon}\right)}, \tag{20}$$

$$G \approx -c + \sum_{n=1}^{\infty} c_n e^{\left(-\frac{c\alpha n}{\epsilon}\right)}, \tag{21}$$

$$P - P_0 \approx \sum_{n=1}^{\infty} d_n e^{\left(-\frac{c\alpha n}{\epsilon}\right)}. \tag{22}$$

Assuming $E'(0) = a$ and $F'(0) = b$ and using conditions given in equation (18) we derive values of higher derivatives at zero, thus initial values are given by

$$\begin{cases} E(0) = 0; \quad E'(0) = a; \quad E''(0) = \frac{-1}{\epsilon(1-\overline{\beta})}; \quad E'''(0) = \frac{-2b}{\epsilon(1-\overline{\beta})}; \\ F(0) = 1; \quad F'(0) = b; \quad F''(0) = 0; \quad F'''(0) = \frac{2a}{\epsilon}; \\ G(0) = 0; \quad G'(0) = 0; \quad G''(0) = -2a; \quad G'''(0) = \frac{2}{\epsilon(1-\overline{\beta})}; \\ P(0) = 0; \quad P'(0) = \frac{-2a(1-\overline{\beta})}{\epsilon}; \quad P''(0) = \frac{2}{\epsilon^2}; \quad P'''(0) = \frac{4b}{\epsilon^2}. \end{cases} \tag{23}$$

For the flow of rotating disk, Cochran calculated the values of a, b, c as $0.54, -0.62$ and 0.886 respectively [9] which are used in equation (23). By considering 4^{th} order approximation for series we calculate the coefficients a_i, b_i, c_i and d_i where $i = 1,2,3$ and 4 which are listed in the Table 1

Table 1: Coefficients of variables for $\overline{\beta} = 0.5$

Coefficients	$\epsilon = 0.01$	$\epsilon = 0.02$	$\epsilon = 0.03$
a_1	-0.01177	-0.02338	-0.03490
a_2	0.04389	0.08732	0.13046
a_3	-0.04637	-0.09232	-0.13794
a_4	0.01426	0.02837	0.04238
b_1	3.96969	3.94204	3.90928
b_2	-5.93358	-5.87301	-5.80130
b_3	3.95108	3.90651	3.85377
b_4	-0.98719	-0.97554	-0.96175
c_1	3.54389	3.54348	3.54302
c_2	-5.31573	-5.31475	-5.31367
c_3	3.54380	3.54305	3.54229
c_4	-0.88596	-0.88578	-0.88563
d_1	1.17465	1.16871	1.16276
d_2	-4.38323	-4.36541	-4.34758
d_3	4.63304	4.61522	4.59739
d_4	-1.42446	-1.41852	-1.41257

Substituting the values from the above Table 1 in the equations (19) - (22) we obtain the solutions for velocity components and pressure for different values of porosity and material parameter.

Case 2: The constant magnetic field in axial direction.

That is $\vec{H} = (0,\ 0,\ H_0)$

For this case, equations (1) and (2) becomes:

$$\begin{aligned} &-\frac{1}{\rho}\frac{\partial p}{\partial r} - \frac{H_0\beta^2\overline{\mu}}{2\epsilon}\left[\frac{\partial^2 v_r}{\partial z^2} - \frac{\partial^2 v_z}{\partial z \partial r}\right] \\ &+\frac{\nu}{\epsilon}\left[\frac{\partial^2 v_r}{\partial r^2} + \frac{\partial}{\partial r}\left(\frac{v_r}{r}\right) + \frac{\partial^2 v_r}{\partial z^2}\right] \quad = \frac{1}{\epsilon^2}\left[v_r\frac{\partial v_r}{\partial r} + v_z\frac{\partial v_r}{\partial z} - \frac{v_\theta^2}{r}\right], \end{aligned} \tag{24}$$

$$\frac{H_0\beta^2\overline{\mu}}{2\epsilon}\left[\frac{\partial^2 v_\theta}{\partial z^2}\right]+\frac{\nu}{\epsilon}\left[\frac{\partial^2 v_\theta}{\partial r^2}+\frac{\partial}{\partial r}\left(\frac{v_\theta}{r}\right)+\frac{\partial^2 v_\theta}{\partial z^2}\right]=\frac{1}{\epsilon^2}\left[v_r\frac{\partial v_\theta}{\partial r}+v_z\frac{\partial v_\theta}{\partial z}+\frac{v_r v_\theta}{r}\right], \tag{25}$$

$$\begin{aligned}&-\frac{1}{\rho}\frac{\partial p}{\partial z}+\frac{H_0\beta^2\overline{\mu}}{2\epsilon}\left[\left(\frac{\partial^2 v_r}{\partial r\partial z}-\frac{\partial^2 v_z}{\partial r^2}\right)+\frac{1}{r}\left(\frac{\partial v_r}{\partial z}-\frac{\partial v_z}{\partial r}\right)+\left(\frac{\partial^2 v_r}{\partial r\partial z}-\frac{\partial^2 v_z}{\partial r^2}\right)\right]\\&+\frac{\nu}{\epsilon}\left[\frac{\partial^2 v_z}{\partial r^2}+\frac{1}{r}\frac{\partial v_z}{\partial r}+\frac{\partial^2 v_z}{\partial z^2}\right]=\frac{1}{\epsilon^2}\left[v_r\frac{\partial v_z}{\partial r}+v_z\frac{\partial v_z}{\partial z}\right],\end{aligned} \tag{26}$$

$$\frac{\partial v_r}{\partial r}+\frac{v_r}{r}+\frac{\partial v_z}{\partial z}=0. \tag{27}$$

The equations (24) to (27) reduces to the ordinary non-linear differential equations by using Von Karman transformations which are given as follows:

$$\epsilon[1-\overline{\beta}]E''-E^2+F^2-GE'=0, \tag{28}$$

$$\epsilon[1-\overline{\beta}]F''-GF'-2EF=0, \tag{29}$$

$$\epsilon^2P'-\epsilon G''-2\overline{\beta}\epsilon E'+GG'=0, \tag{30}$$

$$G'+2E=0. \tag{31}$$

Corresponding boundary conditions are obtained from equation (12)

$$E(0)=0, F(0)=1, G(0)=0, E(\infty)=0, F(\infty)=0, G(\infty)=-c. \tag{32}$$

The system of ordinary differential equations $(28)-(31)$ are expanded through Cochran expansion. With the values of $E'(0)=a$ and $F'(0)=b$, as mentioned in [9] we get the values of higher derivatives at zero as follows:

$$\begin{cases}E(0)=0; \quad E'(0)=a; \quad E''(0)=\frac{-1}{\epsilon(1-\overline{\beta})}; \quad E'''(0)=\frac{-2b}{\epsilon(1-\overline{\beta})};\\ F(0)=1; \quad F'(0)=b; \quad F''(0)=0; \quad F'''(0)=\frac{2a}{\epsilon(1-\overline{\beta})};\\ G(0)=0; \quad G'(0)=0; \quad G''(0)=-2a; \quad G'''(0)=\frac{2}{\epsilon(1-\overline{\beta})};\\ P(0)=0; \quad P'(0)=\frac{-2a(1-\overline{\beta})}{\epsilon}; \quad P''(0)=\frac{2}{\epsilon^2}; \quad P'''(0)=\frac{4b}{\epsilon^2}.\end{cases} \tag{33}$$

The calculated values of a, b, c as $0.54, -0.62$ and 0.886 respectively [9] are substituted in equation (33) and considering 4^{th} order approximation for series the values are listed in Table 2 for the coefficients a_i, b_i, c_i and d_i where $i=1,2,3$ and 4.

Table 2: Coefficients of variables for $\overline{\beta} = 0.5$

Coefficients	$\epsilon = 0.01$	$\epsilon = 0.02$	$\epsilon = 0.03$
a_1	-0.01177	-0.02338	-0.03490
a_2	0.04389	0.08732	0.13046
a_3	-0.04637	-0.09232	-0.13794
a_4	0.01426	0.02837	0.04238
b_1	3.96972	3.94214	3.90951
b_2	-5.93366	-5.87332	-5.80200
b_3	3.95116	3.90682	3.85447
b_4	-0.98722	-0.97564	-0.96199
c_1	3.54389	3.54356	3.54300
c_2	-5.31573	-5.31495	-5.31363
c_3	3.54380	3.54323	3.54225
c_4	-0.88596	-0.88583	-0.88562
d_1	1.17465	1.16871	1.16276
d_2	-4.38323	-4.36541	-4.34758
d_3	4.63304	4.61522	4.59739
d_4	-1.42446	-1.41852	-1.41257

The values for velocity components and pressure are obtained for different values of porosity ϵ and material constant $\overline{\beta}$ by substituting the values from Table 2 in equations $(19) - (20)$.

For the constant magnetic fields in radial and axial direction, the boundary layer displacement thickness are calculated as

$$d = \frac{1}{r\omega}\int_0^\infty v_\theta dz = \int_0^\infty F(\alpha)d\alpha. \tag{34}$$

The displacement thickness are $0.0233988, 0.0465677$ and 0.0695071 for values of $\epsilon = 0.01, 0.02$ and 0.03 respectively for constant magnetic field in radial direction and 1.32657, 1.1054 and 0.908639 for $\epsilon = 1.5, 2.5$ and 3.5 respectively.

Total volume flowing outward z-axis for both cases

$$\begin{aligned} Q = 2\Pi R \int_{z=0}^{\infty} v_r dz \quad &= 2\Pi R^2 \int_0^{\infty} \omega E(\alpha) \sqrt{\frac{\nu}{\omega}} d\alpha, \\ &= -\pi R^2 \sqrt{\omega\nu} G(\infty), \\ &= 2.786094 R^2 \sqrt{\nu\omega}, \\ &= 2.786094 R^2 \nu \frac{\alpha}{z}. \end{aligned}$$

The total volume flowing outward the z- axis are proportional to the dimensionless parameter α.

4. RESULTS AND DISCUSSION

The graphs demonstrates the effects of porosity parameter ϵ and material constant $\overline{\beta}$ on the velocity profiles and pressure. Figure 2 represents radial velocity for different values of porosity and for fixed material constant $\overline{\beta} = 0.5$. The graph for both the cases are similar. The radial velocity increases and decreases, then converges to zero. The rate of convergence slows down with increasing porosity.

Figure 3 and 4 represents tangential velocity for different values of porosity. The graph depicts that for small values of $\epsilon = 0.01, 0.02$ and 0.03, the graph coincide for both cases where as for the higher values of $\epsilon = 1.5, 2.5$ and 3.5 represents the difference in the tangential velocity. For both cases the tangential velocity decreases with increasing values of porosity and the tangential velocity tends to more negative region in case (1) as compared to case (2). On comparing these graphs, the porous medium results in decreasing the convergence rate.

Figure 5 represents the axial velocity for different values of porosity. The axial velocity decreases and tends to a finite negative value -0.886 with increasing values of ϵ. The graphs coincide in both cases.

Figure 6 represents the pressure profile for varying porosity. The pressure decreases and further increases, then converges to zero in both the cases replicating the reverse process has in figure 2. In each case the increasing porosity slows done the rate of convergence.

Figure 9-11 represents radial velocity for $\epsilon = 0.01,0.02$ and 0.03 respectively for varying values of $\overline{\beta}$. The graphs depicts, radial velocity increases with increasing values of material constant and further decreases for further increase in material constant. Thus both porosity and material constant affects the radial velocity.

Figure 12 represents tangential velocity for varying values of material constant for $\epsilon = 0.03$. The graph depicts that material constant does not affect the tangential velocity when a constant magnetic field is considered in radial direction.

Figure 13 represents the axial velocity for varying material constant and for $\epsilon = 0.01$. The graph reveals that increase in the material constant has no effect on the axial velocity when a constant magnetic field is considered in radial direction.

Figure 14-16 represents pressure for varying material constant $\overline{\beta}$ for $\epsilon = 0.01,0.02$ and 0.03 respectively. From graphs it is clear that the pressure increases with increasing material constant but decreases the convergence rate.

Figure 17 represents effect of material constant on tangential velocity for a fixed value of $\epsilon = 2.5$. The tangential velocity decreases smoothly and tends to negative region for increasing values of $\overline{\beta}$. In the close region of disk the smoothness disappears and we observe fluctuation.

In comparison with Benton's and Paras Ram's case radial velocity, tangential velocity, axial velocity and Pressure has following values at $\alpha = 0.1$ for $\epsilon = 0.01$ and $\overline{\beta} = 0.1$ are listed in Table 3.

Table 3: Comparison of velocity profiles and pressure with Benton and Paras Ram

	Benton	Paras Ram	present work(case 1 and case 2)	
Radial velocity	0.0462	0.00000104	0.0000007	0.0504418
Tangential velocity	0.9386	0.000563	0.0005634	0.938128
Axial velocity	-0.0048	-0.8855	-0.88559	-0.005146
Pressure	0.0925	-0.0002082	0.00013	-0.06053

From Table 3 for the present work we infer that the difference in radial velocity and pressure compared to Benton and Paras Ram are due to the effect of porosity and material constant. The tangential velocity and axial velocity values remains same as in Paras Ram case implying that material constant as negligible effect on tangential velocity and axial velocity for constant magnetic field in radial direction. For the constant magnetic field in axial direction, for values of $\epsilon > 1$ we obtain values for velocity profiles approximately equal to Benton case where as observe difference in pressure.

Jenkins model has applications involving bearing system, in order to increase the effective performance of the bearing system by reducing friction. Examples involve water pumps, record players and generators. It is applicable for problems in chemical engineering which involve chemical reaction at the walls of pipes.

5 GRAPHS

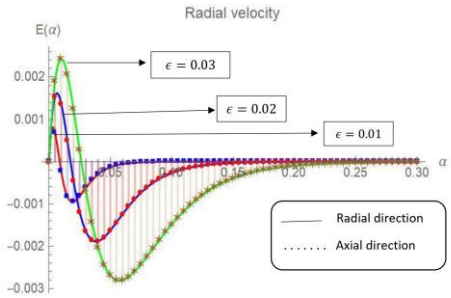

Figure 2: Radial velocity versus α for $\overline{\beta} = 0.5$

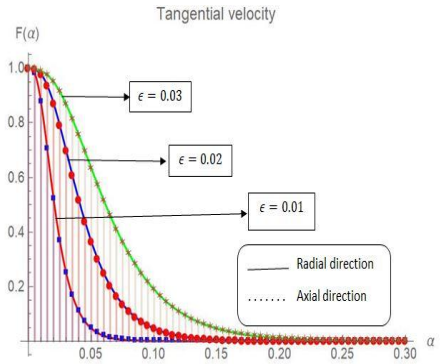

Figure 3: Tangential velocity versus α for $\overline{\beta} = 0.5$

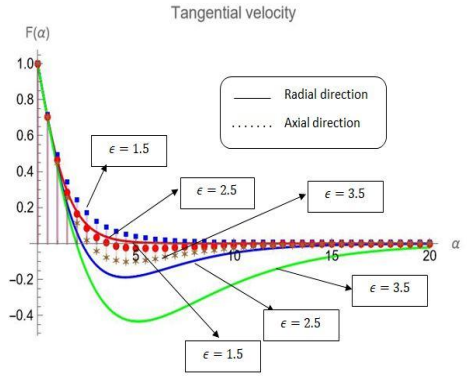

Figure 4: Tangential velocity versus α

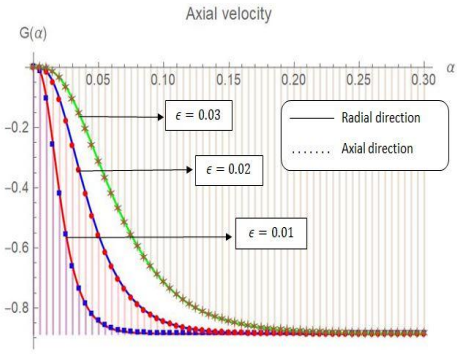

Figure 4: Axial velocity versus α for $\overline{\beta} = 0.5$

for $\overline{\beta} = 0.5$

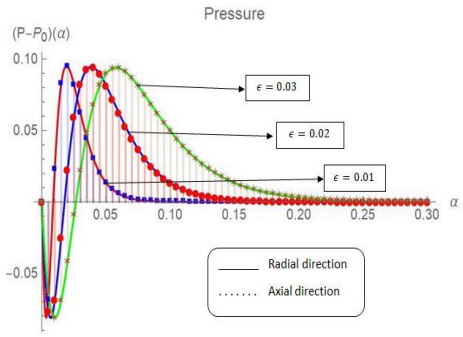

Figure 6: Pressure versus α for $\overline{\beta} = 0.5$

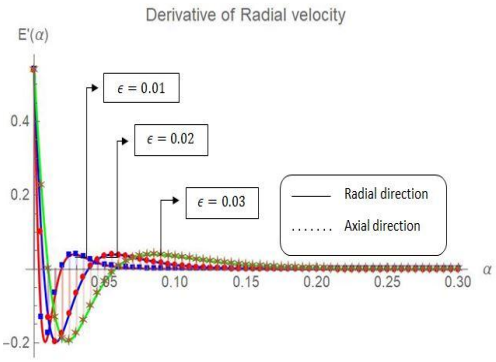

Figure 7: Derivative of Radial velocity versus α for $\overline{\beta} = 0$

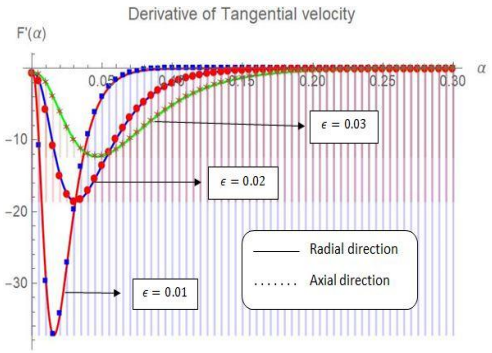

Figure 8: Derivative of Tangential velocity $\overline{\beta} = 0.5$

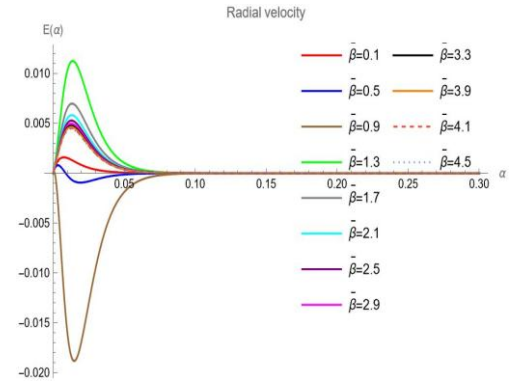

Figure 9: Radial velocity for varying values versus α for of $\overline{\beta}$ at $\epsilon = 0.02$

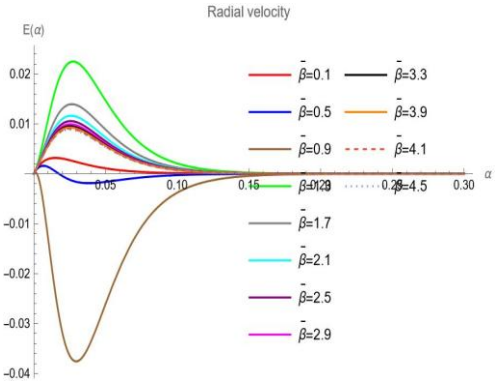

Figure 10: Radial velocity for varying values of $\overline{\beta}$ at $\epsilon = 0.02$

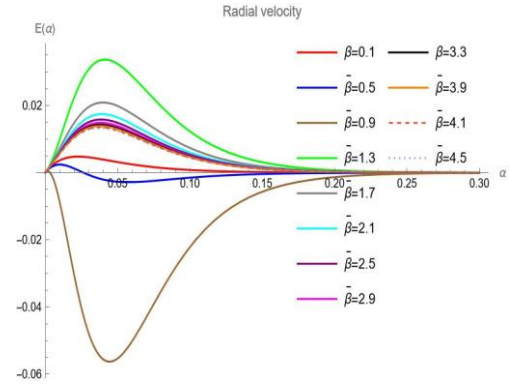

Figure 11: Radial velocity for varying values of $\overline{\beta}$ at $\epsilon = 0$.

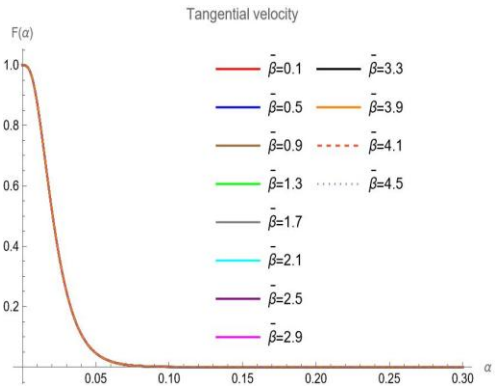

Figure 12: Tangential velocity for varying values of $\overline{\beta}$ at $\epsilon = 0.01$.

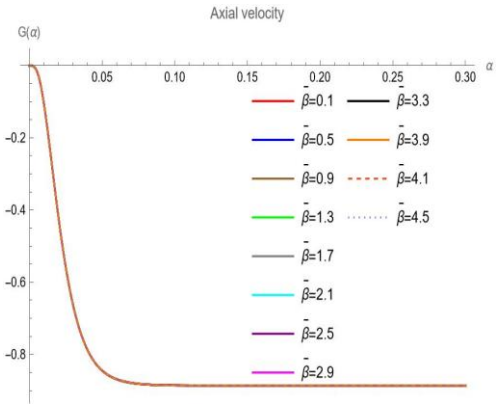

Figure 13: Axial velocity for varying values of $\overline{\beta}$ at $\epsilon = 0.01$

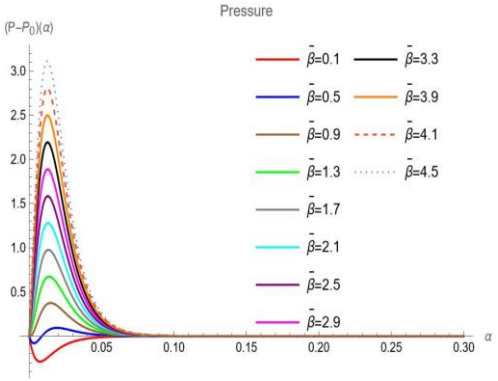

Figure 14: Pressure for varying values of $\overline{\beta}$ at $\epsilon = 0.01$

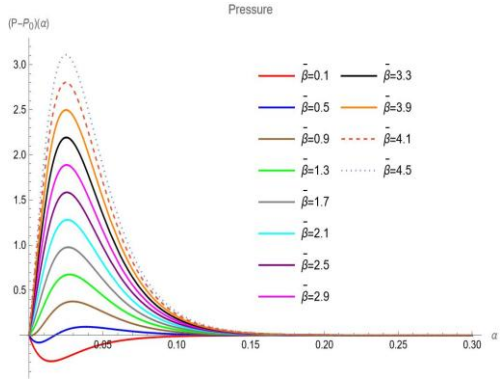

Figure 15: Pressure for varying values of $\overline{\beta}$ at $\epsilon = 0.02$

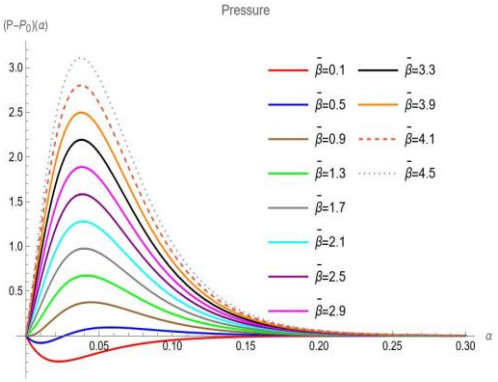

Figure 16: Pressure for varying values $\epsilon = 0.03$

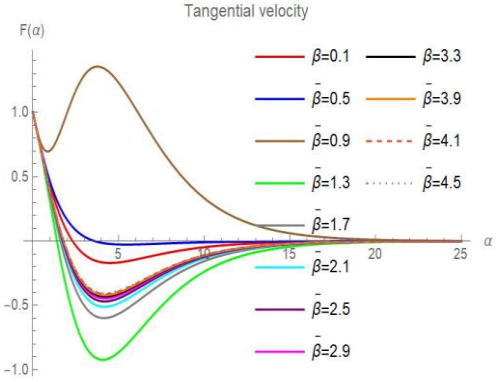

Figure 17: Tangential velocity for varying values of $\overline{\beta}$ at of $\overline{\beta}$ at $\epsilon = 2.5$

6. REFERENCES

1. Rosensweig, R. E., Ferrohydrodynamics, Dover Publications, Cambridge University Press,1985.
2. Achala, L. N. and Asha, C.S., "Analysis of flow of polar and non polar incompressible ferrofluids",

Journal of Advances in Physics, Vol. 10, No.2, 2015, 2733-2740.
3. Scherer, C. and Figueiredo Neto, A. M., "Ferrofluids: Properties and Applications", Brazilian Journal of Physics, vol. 35, no.3A, 2005,718-727.
4. Neuringer, J. L. and Rosensweig, R. E., Magnetic Fluids, Physics of Fluids, Vol. 7, No. 12, 1964,1927-1937.
5. Paras Ram and Kushal Sharma, "On the Revolving Ferrofluid Flow Due to Rotating Disk", International Journal of Nonlinear Science, Vol. 13, No.3, 2012, pp. 317-324.
6. Paras Ram, Anupam Bhandari and Kushal Sharma., "Axi-symmetric Ferrofluid Flow with Rotating Disk in a Porous Medium", International Journal of Fluid Mechanics,2(2), 2010, 151-161.
7. Ram, P., Sharma, K. and Bhandari, A., "Effect of Porosity on Ferrofluid Flow with Rotating Disk", International Journal of Applied Mathematics and Mechanics, Vol. 6, No. 16, 2010, 67-76.
8. Karman, V., "Uber laminare and turbulente Reibung", Zeitschrift für Angewandte Mathematik und Mechanik, Vol. 1, No. 4, 1921, 232-252.
9. Cochran, W. G., "The Flow Due to a Rotating Disk", Mathematical Proceedings of the Cambridge Philosophical Society, Vol. 30, No. 3, 1934, 365-375.
10. Benton, E. R., "On the Flow Due to a Rotating Disk, Journal of Fluid Mechanics", Vol. 24, No. 4, 1966, 781-800.
11. Verma, P.D.S. and Singh, M., "Magnetic Fluid flow through porous annulus", Int. J. Non-Linear Mechanics, 16 (3/4),1979, 371-378.
12. Attia, H. A., "Rotating disk flow and heat transfer through a porous medium of a non-Newtonian fluid with suction and injection", Communications in Nonlinear Science and Numerical Simulation, 13(8),2008, 1571–1580.
13. Paras Ram and Anupam Bhandari, "Flow Characteristics of Revolving Ferrofluid with Variable Viscosity in a Porous Medium in the Presence of Stationary Disk", Fluid Dynamics and Materials Processing, vol.8, no.4, 2012, 437-451.
14. Attia, H.A., "Effect of Porosity on Unsteady Couette Flow with Heat Transfer in the Presence of Uniform Suction and Injection", Mechanics and Mechanical Engineering, Vol. 13, No. 1 2009, 85–90.
15. Paras Ram and Kushal Sharma., "Revolving Ferrofluid Flow under the Influence of MFD Viscosity and Porosity with Rotating Disk", Journal of Electromagnetic Analysis and Applications, Vol. 3 No. 9 ,2011 , Article ID: 7463.
16. Bhandari, A. and Kumar, V., "Effect of Porosity and Magnetic Field Dependent Viscosity on Revolving Ferrofluid Flow in the Presence of a Stationary Disk", Fluid Dynamics and Materials Processing, vol.10, no.3, 2014, 359-375.
17. Barnoon, P., Toghraie, D. and Karimipour, A., "Application of rotating circular obstacles in improving ferrofluid heat transfer in an enclosure saturated with porous medium subjected to a magnetic field", Journal of Thermal Analysis and Calorimetry, 2020.
18. Shah, R. C. and Bhat, M. V., "Ferrofluid lubrication of a slider bearing with a circular convex pad", J.Natn.Sci.Foundation, sri Lanka, 32(3 and 4),2004, 139-148.
19. Paras ram and Verma, P. D. S., "Ferrofluid lubrication in porous inclined slider bearing",Indian journal of pure applied Math, 30(12), 1999, 1273-1281.
20. Agrawal, V. K., "Magnetic-fluid-based porous inclined slider bearing", Wear, 107(2),1986, 33–139.
21. Rajesh, C.S. and Bhat, M.V., " Ferrofluid lubrication of a parallel plate squeeze film bearing", Theoret. Appl. Mech., Vol.30, No.3, 2003, 221-240.
22. Mishra, S. R., Barik, M. and Dash, G. C., "An analysis of hydrodynamic ferrofluid lubrication of an inclined rough slider bearing", Tribology - Materials, Surfaces and Interfaces, 12(1),2018, 17–26.
23. Jimit, R. P. and Deheri, G. M., "Jenkins Model based ferrofluid lubrication of a curved rough annular squeeze film: Effect of slip velocity", Theoretical and Applied Mechanics, Vol.(42), Issue 1, 2015, 53-71.
24. Asha, C.S. and Achala, L. N., " Ferroluid lubrication for rough and smooth surface slider bearing with and without squeeze velocity", GE-International Journal of Engineering Research, Vol. 4, Issue 8,2016, pp.59-69.